Nanoscale

Accepted Manuscript

Nanoscale

ARTICLE

Elaborately designed diblock nanoprobes for simultaneous multicolor detection of microRNAs†

Chenguang Wang, ‡ [a] Huan Zhang, ‡ [a] Dongdong Zeng ‡ [a], Wenliang Sun [b], Honglu Zhang [b], Ali Aldalbahi [c], Yunsheng Wang [a], Lili San [a], Chunhai Fan [b], Xiaolei Zuo *[b], Xianqiang Mi *[a]

Simultaneous detection of multiple biomarkers has important prospects in biomedical field. In this work, we demonstrated a novel strategy for detection of multiple microRNAs (miRNAs) based on gold nanoparticles (Au NPs) and poly adenine (polyA) mediated nanoscale molecular beacon (MB) probes (named p-nanoMBs). Novel fluorescent labeled p-nanoMBs bearing consecutive adenines were designed, of which a polyA served as an effective anchoring block binding to the surface of Au NPs, and the appended hairpin block formed an upright conformation that favored the hybridization with targets. Through the co-assembling method and the improved hybridization conformation of the hairpin probes, we achieved high selectivity for specifically distinguishing DNA targets from single-base mismatched DNA targets. We also realized multicolor detection of three different synthetic miRNAs in a wide dynamic range from 0.01 nM to 200 nM with a detection limit of 10 pM. What's more, we even detected miRNAs in a simulated serum environment, which indicated that our method could be used in complex media. Compared with traditional method, our strategy provide a promising alternative method for qualitative and quantitative detection of miRNAs.

Introduction

It is of great importance to develop rapid, sensitive, and cost-effective bioassay methods in life sciences and medical fields.[1-3] Molecular beacon (MB) is a stem-and-loop oligonucleotide, which was dual labeled with a fluorophore and a quencher group on each end.[4] The target can bind to the loop region and competitively force apart the fluorophore and the quencher,

generating a fluorescence signal.[4,5] Therefore, MB can serve as a promising molecular analytical tool.[6-8] It is reported that MB probes have many advantages, such as high signal-to-background ratios, sensitive to the target and high sequence specificity.[9] Hence, it has a broad applications in biosensing, biomedical detection, and even in rapid clinical diagnostics fields.[10-13] However, traditional MB probes have some inadequacies such as low efficiency of the quencher and instability of the stem-loop structure, which limited their further application.[14,15] Recently, nanoscale MBs (nanoMBs) using nanomaterials (e.g. carbon nanotubes, graphene oxide nanosheets or gold nanoparticles) as quenchers have attracted considerable attentions.[16-18] Among which, gold nanoparticles (Au NPs) are frequently used not only because they possess distinct optoelectronic and catalytic properties, but they exhibit ultrahigh fluorescence quenching ability.[19-24] As early as in 2001, Dubertret et al. designed a Au NPs-based MB using 1.4

[a.] *Laboratory of System Biology, Shanghai Advanced Research Institute, Chinese Academy of Sciences, Shanghai 201210, China.E-mail: mixq@sari.ac.cn.*
[b.] *Division of Physical Biology and Bioimaging Center, Shanghai Synchrotron Radiation Facility, Shanghai Institute of Applied Physics, Chinese Academy of Sciences, Shanghai 201800, China.E-mail: zuoxiaolei@sinap.ac.cn.*
[c.] *Chemistry Department, King Saud University, P. O. Box 2455, Riyadh 11451, Saudi Arabia.*
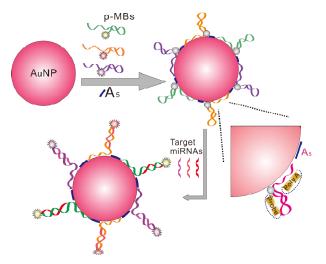
nm diameter Au NPs as quenchers with the sensitivity enhanced up to 100-fold.[14] Fan and co-workers constructed a multicolor nanoMBs for DNA detection by use of relatively large Au NPs (15nm), which could instantaneously detect three types of tumor-suppressor genes.[25] Tang et al. constructed a multicolor MB probes which could be used for simultaneous detection and imaging of four types of mRNAs in living cells.[26]

So far, the construction of Au NPs based nanoMB probes mainly depended on assembling thiolated DNAs to the surface of Au NPs, which employed a classical process with the time-consuming salt-aging protocol for about 1-2 days.[27,28] To simplify, Liu and his coworkers functionalized gold nanoparticles with thiolated DNA using a fast pH-assisted route, which showed a synergistic effect between pH and salt in forming DNA-Au NPs complex.[29] However, the above two protocols have similar shortcomings where the conformation and orientation of the probe could not be accurately controlled and the hybridization efficiency was relatively low.[30] Poly adenine (polyA) was a kind of newly reported linkers between Au NPs and DNA oligonucleotides, which possessed similar affinity with the thiol group but offered a much higher controllability for the orientation of DNAs assembled at the surface of Au NPs.[31,32] What's more, the surface density of polyA mediated diblock DNA oligonucleotides could be facilely modulated by simply varying the length of polyA, meanwhile the hybridization efficiency could be controlled and improved.[33] Besides, they were free of modification during the synthesis which in turn reduced the cost.

Herein we reported a novel strategy for construction of multicolor nanoprobes based on Au NPs and polyA mediated diblock hairpin MBs (named p-MBs) for detection of miRNAs. As shown in Scheme 1, polyA block of the p-MBs bound tightly to the surface of Au NPs, and the hairpin block stood upright at the surface of Au NPs. To the best of our knowledge, it is the first time that fluorescent labeled diblock p-MBs with consecutive adenines were designed as probes for miRNA detection. During our study, we employed 13nm Au NPs to load three different dyes labeled p-MBs by a facile pH-assistant method.[34] Moreover, we improved our method by co-assembling short oligo-As (A$_5$) with p-MBs for higher stability and hybridization efficiency. Meanwhile, we redesigned the hybridization conformation of the p-MBs by making the stem section

partially hybridize with the target to further improve the sensitivity and selectivity for miRNA detection. Our results showed that the Au NPs based p-MB nanoprobes (named p-nanoMBs) can synchronously discriminate three different miRNAs with a detection limit of 10pM. Meanwhile, our probes also exhibited good performance in simulated serum samples.

Scheme 1. Illustration of the multicolor p-nanoMBs for detection of three miRNA targets.

Results and discussion

Design and Construction of p-nanoMBs. At first, we optimized the assembling condition of p-MBs with Au NPs using single color probe, where 5'-end of p-MB1 was labeled with FAM and 3'-end modified with twenty adenines. Distinct from the hybridization conformation of original MB probe (target binds in the loop region of the original MB), the structure of our probe was designed with the 5'-stem sequence partially complementary to the target sequence to gain higher fluorescent signal (Fig. 1a). However, we found that p-MB1 assembled Au NPs occasionally aggregated in salt, and the background is relatively high before hybridizing with the target. In order to solve the problem, we improved the assembling protocol by introduction of short oligo-As (5 As, named A$_5$) to co-assemble with p-MB1. From Fig. 1b, we could see that the fluorescent signal was about 9 times higher than that without A$_5$. We attributed it to that A$_5$ could fill in the gaps at the surface of Au NPs where polyA could not cover, thus increased the stability and obtained better signal to background ratio. The dynamic light scattering (DLS) analysis data provided more solid evidence (Fig. S1†).

The hydrodynamic diameters of Au NPs alone and Au NPs assembled with A_5 didn't show much difference, which indicated that polyA preferentially adsorbed and lay flat on Au NP surface. As a comparison, Au NPs co-assembled with p-MB1 and short A_5 had the largest hydrodynamic diameter of 45.8nm, while the hydrodynamic diameter of p-MB1 assembled Au NPs was only 35.7 nm. The difference (~10nm) between them suggested that the co-assembling method did make the hairpin block form a more upright and extended conformation that benefited the hybridization.
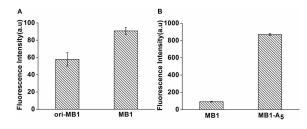

Fig. 1 The fluorescent changes for designing and constructing single color p-nanoMB. A: Fluoresent signal of original MB1 (ori-MB1, the loop region was completely complemented to the target) and the new p-MB1 (MB1, the 5'stem sequence was partially complemented to the target). B: Fluoresent signal of assembling p-nanoMBs with (A_5) or without (no-A_5) short oligonucleotides. The ratio between the hairpin probe1 and A_5 was 3:1 (final concentration ratio).

More interestingly, we found that the ratio between the p-MBs and the A_5 during the co-assembly played an important role for the subsequent detection. As shown in Fig. S2†, the ratio of 3:1 (final concentration ratio) between p-MBs and A_5 exhibited strongest fluorescent signal than higher (e.g. 10:1 or 5:1) or lower (e.g. 1:3 or 1:2) ratios after hybridization with the targets. Therefore, the ratio of 3:1 was employed for preparation of p-nanoMBs and further detection experiments.

We then constructed multicolor p-nanoMBs with three different fluorophores labeled probes. By following a well-established fluorescence assay protocol,[35] we found that each 13nm Au NP carried about ~21 FAM labeled p-MB1, ~20 ROX labeled p-MB2, and ~22 Cy5 labeled p-MB3 (details of the information were given in Fig. S3† of the Supporting Information). From TEM images in Fig. 2, we found that both the naked Au NPs and the p-nanoMBs were uniform distributed, which indicated the successful assembling

of our probes on the surface of Au NPs. The UV-vis absorption spectra (Fig. S4†) showed that the maximum absorption peak of the Au NPs was slightly red-shifted from 519 nm to 525 nm after the assembly, which also confirmed that the Au NPs were successfully functionalized with p-MB probes.
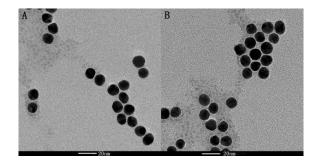

Fig. 2 TEM images: A: AuNPs. B: the P-nanoMBs. Scale bars are 20 nm.

Selectivity study of the p-nanoMBs using DNA Targets as model. To further evaluate the potential application of the p-nanoMBs for simultaneously multicolor detection of miRNAs, we first employed DNA targets (the sequences were shown in Table S1†) to establish our method. Three different dye labeled p-MB probes were co-assembled to Au NPs for detection of DNA targets. Single-base mismatched DNA strands were tested under the same condition to evaluate the discrimination ability of our probes. Results (Fig. 3) demonstrated that a significant fluorescent enhancement was observed after addition of DNA targets (with a final concentration of 200nM for each) , which led to 9.0-fold, 9.2-fold, and 13-fold higher fluorescent signal for FAM-labeled, ROX-labeled and Cy5-labeled p-nanoMBs respectively, comparing to the background . In contrast, the fluorescent signals of single-base mismatched DNA strands did not change obviously. This significant differences demonstrated that our p-nanoMBs were efficient in discriminating specific targets and retained high sequence specificity. We believed that this feature benefited from the conformational constraint of hairpin structure, which could be used for more challenging applications such as allele discrimination.

pancreatic cancer.[41,42] In the light of our above study, herein we constructed multicolor p-nanoMBs for detecting three types of synthetic miRNAs (miRNA-155, miRNA-196a, and miRNA-210), where the p-MB probes were labeled with FAM, Rox, and Cy5, respectively. Interestingly, we found that our p-nanoMBs responded specifically to the corresponding targets, and the characteristic fluorescent signal peaks showed negligible cross-talk. As shown in Fig. 4, the fluorescence intensity increased proportionally with the miRNA target concentration from 0.01 nM to 200 nM with a well concentration-dependent linear curve from 0.01 nM to 10 nM (inset of Fig. 4). It is worth noting that the p-nanoMBs possessed a wide dynamic range (3 orders of magnitude) for detection of miRNAs with a quite low detection limit (10pM, >3SD), which was 50 times higher than previous reported multicolor nanobeacons.[25] This improvement could be attributed to our co-assembly strategy and the novel design of hybridization conformation of our probes towards the targets. The selectivity of the p-nanoMBs towards different miRNAs was demonstrated in Fig. 5, which exhibited that each fluorescent labeled probe specifically hybridized with the corresponding miRNA target, and caused 5 to 7- fold higher fluorescent signals than other miRNAs. These above results demonstrated that the p-nanoMBs could effectively distinguish specific miRNA targets as well as single-base mismatched DNA targets, implying that the p-nanoMBs possessed high sequence specificity and selectivity towards miRNA targets.
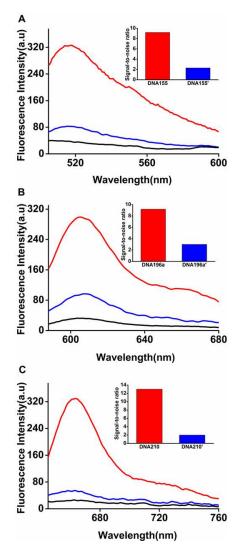
Fig. 3 Multiplexed detection of DNA targets using the p-nanoMBs. The p-nanoMBs (1 nM, black curve) were hybridized with three different perfectly matched DNA targets (red curve) and single-base mismatched DNA targets (blue curve) with the final concentration of 200 nM. A: DNA 155 (FAM labeled, emission at 520 nm). B: DNA 196a (ROX labeled, emission at 607 nm). C: DNA 210 (Cy5 labeled, emission at 670 nm). Inset: the signal to noise ratio of perfectly matched DNA targets (red) and single-base mismatched DNA targets (blue).

Application of p-nanoMBs for multicolor detection of different kinds of miRNAs. Simultaneous detection of related biomarkers is quite significant for early detection of tumor. Accumulated evidences have demonstrated that miRNAs could be used as biomarkers for screening and detecting of early-stage cancer.[36-40] Recently, several miRNAs have already been proven to be able to predict the development of

Nanoscale Accepted Manuscript
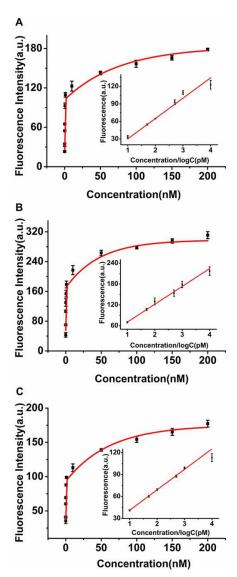
Please do not adjust margins

Fig. 4 The fluorescent intensity curve for the detection of different synthetic miRNA targets with various concentration (0, 0.01, 0.05, 0.1, 0.5, 1, 10, 50, 100, 150 and 200 nM) measured with different excitation wavelength, respectively. A: FAM labeled p-nanoMBs targeting miR155 B: Cy5 labeled p-nanoMBs targeting miR210. C: ROX labeled p-nanoMBs targeting miR196a. Inset: linear detection curve range from 0.01nM to 10nM.

Fig. 5 Specificity of the p-nanoMBs over several miRNA targets. p-nanoMBs (1nM) targeting to different miRNAs were mixed with the target miRNA and three other kinds of miRNAs. A: Target miR155 and other pancreatic cancer related miRNAs (miR196a, miR21 and miR210). B: Target miR196a and other pancreatic cancer related miRNAs (miR210, miR155 and miR21), C: Target miR210 and other pancreatic cancer related miRNAs (miR196a, miR155 and miR21). The concentration of all the miRNAs are 200 nM.

Application of p-nanoMBs for miRNA detection in simulated serum samples. The high selectivity and specificity of this strategy inspired us to detect the target miRNAs in complex samples. We mixed three miRNAs (miR155, miR196a and miR210) with diluted fetal bovine serum (10%). Even though there existed interference of other components in the simulated biological fluids, our preliminary experiments still showed that each kind of p-nanoMB specifically bound

to its own miRNA target and produced a fluorescence signal that was 5 to 7-fold higher (Fig. 6). This proved that our method was able to detect target miRNAs in complex media. This result indicated that the newly designed p-nanoMBs might be a promising candidate for real sample detection and exhibited a great potential in clinical diagnosis.
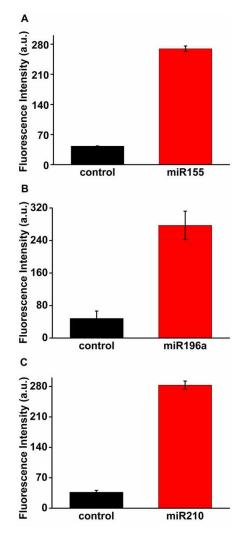

Fig. 6 Serum detection using multicolor p-nanoMBs. A: The p-nanoMBs was mixed with miR155 target, measured with 494 nm excitation wavelength. B: The p-nanoMBs was mixed with miR196a target, measured with 578 nm excitation wavelength. C: The p-nanoMBs was mixed with miR210 target, measured with 633 nm excitation wavelength.

Experimental

Materials. Hydrogen tetrachloroaurate (Ⅱ) (HAuCl$_4$· 4H$_2$O, 99.99%), Trisodium citrate (C$_6$H$_5$Na$_3$O$_7$ · 2H$_2$O),

Phosphate, NaCl, MgCl$_2$, and KCl were purchased from China National Pharmaceutical Group Corporation (Shanghai, China). All the chemicals were of analytic grade and used without further purification. Fetal bovine serum (FBS) was purchased from Sigma-Aldrich. Water used in the experiments was Milli-Q water.

All of the p-MB probes and DNA targets in the experiment were synthesized and HPLC purified by Sangon Biological Engineering (Shanghai China) Co., LTD. And all the miRNAs were synthesized and purified by Invitrogen Company. See details in Table S1.

Instruments. Transmission electron microscopy (TEM) was carried out on a JEM-100CX II electron microscope. Absorption spectra were measured on a UV-Vis spectroscopy (U-3010 UV-Vis spectroscopy, Hitachi, Tokyo, Japan). Fluorescence spectra were collected by a fluorescence spectrometer (F-900, Edinburgh Instruments Ltd, British). Hydrodynamic diameters were measured by Delsa™Nano Submicron Particle Size and Zeta potential Particle Analyzer (Beckman Coulter Inc, United States). All pH measurements were performed with a digital pH-meter (FE20, Mettler-Toledo, Shanghai, China).

Preparation of Gold Nanoparticles. The 13nm Au NPs was synthesized through citrate acid reduction method.[43] In brief, 100mL HAuCl$_4$ (0.01%) was stirred rapidly and heated to boiling, then 3.5mL trisodium citrate (1%) was injected into the HAuCl$_4$ solution. The mixed solution was kept boiling and stirring for another 20 minutes, then gradually cooled to room temperature. The obtained Au NPs solution was filtered through a 0.22μm millipore membrane filter and stored at 4°C for further use. Transmission electron microscopy (TEM) images were used to measure the particle sizes.

Prediction of PolyA Mediated p-MBs Structure. The potential secondary structures of hairpin DNA probes were predicted using NUPAK (http://www.nupack.org/). It indicated that all three probes had formed "stem and loop" conformation.

Preparation of the p-nanoMBs. To prepare the polyA block mediated DNA-AuNPs conjugates, the main procedure included four steps. First, p-MB probes and oligo-As (A$_5$) were added to an Au NPs solution (10nM) to reach final concentrations of 3μM and 1μM, respectively. Second, citrate·HCl buffer (pH=2, 500mM) was added to the mixed solution to reach a final concentration of 10mM. After slight vortex mixing, the mixture was incubated at room temperature for 3 min. Then, the pH of the solution was adjusted back to neutral by adding 200 mM PB buffer (pH 7.6, 3μL buffer for 50μL AuNP solution) and incubated for another 5-10 min at room temperature. Finally, the mixture solution was centrifuged at 12000 rpm, and washed three times with 100 mM PB buffer (PH 7.6) to remove the

unassembled probes completely. The final p-nanoMBs solution was redispersed in 100 mM PBS buffer (PH 7.6) for further experiments with a final concentration of 1nM (determined by measuring their emission peak at 524 nm, ε= $2.7×10^8$ L $mol^{-1}cm^{-1}$).

Quantitation of Each Probe Loaded on the p-nanoMBs. The amount of the p-MB probes loaded on Au NPs were quantified by the published protocol.[44] The mercaptoethanol (ME) was added (with a final concentration of 20mM) to the p-nanoMBs solution (final concentration=1nM). After being incubated overnight with shaking at room temperature, the p-MB probes were released from the surface of Au NPs. Then the released probes were separated through centrifugation measured with a fluorescence spectrometer. The fluorescence of FAM-labeled p-MB1 was excited at 494 nm and measured at 520 nm. The fluorescence was converted to molar concentrations of p-MBs by interpolation from a standard linear calibration curve that was prepared with known concentrations of fluorescent DNA with identical buffer pH, ionic strength and ME concentration.

Dynamic Light Scattering (DLS) Measurements. DLS measurements for hydrodynamic diameters of AuNPs, AuNPs-A_5, AuNPs-MB1 and AuNPs-MB1-A_5 (final concentration=1nM) were conducted using Delsa™ Nano Submicron Particle Size and Zeta potential Particle Analyzer, Beckman Coulter, Inc.

Hybridization Experiment. For multiplexed detection, the p-nanoMBs (1nM) containing FAM, ROX, Cy5 colors were incubated with three complementary miRNA targets with increasing concentrations (0, 0.01, 0.05, 0.1, 0.5, 1, 10, 50, 100, 150, 200 nM), respectively. After 1 h at 37°C, the fluorescence was monitored at corresponding condition. All experiments were repeated at least three times.

Specificity Experiment. The complementary DNA or miRNA target for each probe and other targets (mismatch DNA or non-target miRNA) were spiked in 200μL hybridization buffer containing 1nM multicolor p-nanoMBs, with the final concentration of the targets were 200 nM. All experiments were repeated at least three times.

miRNA Detection in Fetal Bovine Serum. For detection of miRNA in diluted fetal bovine serum (FBS), 100μL of FBS with or without additional multicolor p-nanoMBs solution was diluted with 900μL PBS buffer (pH7.6, 100mM). Then three miRNA targets were added to the 200ul diluted FBS (10%), respectively. The final concentration of the targets was 200 nM.

Conclusions

To sum up, we developed a novel probe (p-nanoMBs) based on gold nanoparticles (Au NPs) and polyA mediated diblock hairpin molecular beacons (p-MBs), which could be used for multicolor detection of miRNAs with high selectivity and sensitivity. In our study, we employed polyA block to conjoint with Au NPs through a fast pH assisted assembling method instead of traditional thiolated attachment way, which was simple and low-cost. Short A_5 were introduced to co-assemble with our p-MB probes, which guaranteed the stability and gained better signal to noise. Besides, we redesigned the hybridization conformation of the p-MBs by making stem sequences partially complementary to the targets to improve the sensitivity and selectivity of our probes. Based on this novel design strategy, the p-nanoMB probes could realize multicolor detection of three different pancreatic cancer related miRNAs (miRNA-155, miRNA-196a, and miRNA-210) with a detection limit of 10pM. We also challenged the detection ability of our probes towards more complicated samples, and the results suggested that the p-nanoMBs might be a promising candidate for real sample detection and exhibited a great potential in clinical diagnosis. More importantly, compared to traditional detection of single miRNA biomarker, our approach of multiple detection could offer more comprehensive and reliable information, which is of great importance in early diagnosis.

Acknowledgements

Notes and references

(1) Li, Z. H.; Zhao, B.; Wang, D. F.; Wen, Y. L.; Liu, G.; Dong, H. Q.; Song, S. P.; Fan, C. H. DNA Nanostructure-Based Universal Microarray Platform for High-Efficiency Multiplex Bioanalysis in Biofluids. *Acs Appl. Mater.Inter* **2014**, *6*, 17944-17953.

(2) Shi, H.; Liu, J.; Geng, J.; Tang, B. Z.; Liu, B. Specific detection of integrin alphavbeta3 by light-up bioprobe with aggregation-induced emission characteristics. *Journal of the American Chemical Society* **2012**, *134*, 9569-9572.

(3) Ng, A. H.; Lee, M.; Choi, K.; Fischer, A. T.; Robinson, J. M.; Wheeler, A. R. Digital microfluidic platform for the detection of rubella infection and immunity: a proof of concept. *Clinical chemistry* **2015**, *61*, 420-429.

(4) Tyagi, S.; Kramer, F. R. Molecular beacons: Probes that fluoresce upon hybridization. *Nat Biotechnol* **1996**, *14*, 303-308.

(5) Tyagi, S.; Bratu, D. P.; Kramer, F. R. Multicolor molecular beacons for allele discrimination. *Nat Biotechnol* **1998**, *16*, 49-53.

(6) Tan, W. H.; Wang, K. M.; Drake, T. J. Molecular beacons. *Curr Opin Chem Biol* **2004**, *8*, 547-553.

(7) Wang, K. M.; Tang, Z. W.; Yang, C. Y. J.; Kim, Y. M.; Fang, X. H.; Li, W.; Wu, Y. R.; Medley, C. D.; Cao, Z. H.; Li, J.; Colon, P.; Lin, H.; Tan, W. H. Molecular Engineering of DNA: Molecular Beacons. *Angew Chem Int Edit* **2009**, *48*, 856-870.

(8) Uddayasankar, U.; Krull, U. J. Analytical performance of molecular beacons on surface immobilized gold nanoparticles of varying size and density. *Anal Chim Acta* **2013**, *803*, 113-122.

(9) Marras, S. A. E.; Kramer, F. R.; Tyagi, S. Efficiencies of fluorescence resonance energy transfer and contact-mediated quenching in oligonucleotide probes. *Nucleic Acids Res* **2002**, *30*.

(10) Zheng, J.; Yang, R. H.; Shi, M. L.; Wu, C. C.; Fang, X. H.; Li, Y. H.; Li, J. H.; Tan, W. H. Rationally designed molecular beacons for bioanalytical and biomedical applications. *Chem Soc Rev* **2015**, *44*, 3036-3055.

(11) Zheng, J.; Hu, Y. P.; Bai, J. H.; Ma, C.; Li, J. S.; Li, Y. H.; Shi, M. L.; Tan, W. H.; Yang, R. H. Universal Surface-Enhanced Raman Scattering Amplification Detector for Ultrasensitive Detection of Multiple Target Analytes. *Anal Chem* **2014**, *86*, 2205-2212.

(12) Kim, E.; Yang, J.; Park, J.; Kim, S.; Kim, N. H.; Yook, J. I.; Suh, J. S.; Haam, S.; Huh, Y. M. Consecutive Targetable Smart Nanoprobe for Molecular Recognition of Cytoplasmic microRNA in Metastatic Breast Cancer. *Acs Nano* **2012**, *6*, 8525-8535.

(13) Tyagi, S.; Kramer, F. R. Molecular beacons in diagnostics. *F1000 medicine reports* **2012**, *4*, 10.

(14) Dubertret, B.; Calame, M.; Libchaber, A. J. Single-mismatch detection using gold-quenched fluorescent oligonucleotides (vol 19, pg 365, 2001). *Nat Biotechnol* **2001**, *19*, 680-681.

(15) Tsourkas, A.; Behlke, M. A.; Bao, G. Structure-function relationships of shared-stem and conventional molecular beacons. *Nucleic Acids Res* **2002**, *30*, 4208-4215.

(16) Su, X.; Zhang, C.; Zhao, M. Discrimination of the false-positive signals of molecular beacons by combination of heat inactivation and using single walled carbon nanotubes. *Biosensors & bioelectronics* **2011**, *26*, 3596-3601.

(17) Ryoo, S. R.; Lee, J.; Yeo, J.; Na, H. K.; Kim, Y. K.; Jang, H.; Lee, J. H.; Han, S. W.; Lee, Y.; Kim, V. N.; Min, D. H. Quantitative and multiplexed microRNA sensing in living cells based on peptide nucleic acid and nano graphene oxide (PANGO). *Acs Nano* **2013**, *7*, 5882-5891.

(18) Jain, A.; Reddy-Noone, K.; Pillai, A. K.; Verma, K. K. Conversion to isothiocyanates via dithiocarbamates for the determination of aromatic primary amines by headspace-solid phase microextraction and gas chromatography. *Anal Chim Acta* **2013**, *801*, 48-58.

(19) Katz, E.; Willner, I. Integrated nanoparticle-biomolecule hybrid systems: Synthesis, properties, and applications. *Angew Chem Int Edit* **2004**, *43*, 6042-6108.

(20) Saha, K.; Agasti, S. S.; Kim, C.; Li, X. N.; Rotello, V. M. Gold Nanoparticles in Chemical and Biological Sensing. *Chem Rev* **2012**, *112*, 2739-2779.

(21) Rosi, N. L.; Mirkin, C. A. Nanostructures in biodiagnostics. *Chem Rev* **2005**, *105*, 1547-1562.

(22) Sapsford, K. E.; Berti, L.; Medintz, I. L. Materials for fluorescence resonance energy transfer analysis: Beyond traditional donor-acceptor combinations. *Angew Chem Int Edit* **2006**, *45*, 4562-4588.

(23) Luo, X. L.; Morrin, A.; Killard, A. J.; Smyth, M. R. Application of nanoparticles in electrochemical sensors and biosensors. *Electroanal* **2006**, *18*, 319-326.

(24) Shi, Y. P.; Pan, Y.; Zhang, H.; Zhang, Z. M.; Li, M. J.; Yi, C. Q.; Yang, M. S. A dual-mode nanosensor based on carbon quantum dots and gold nanoparticles for discriminative detection of glutathione in human plasma. *Biosensors & bioelectronics* **2014**, *56*, 39-45.

(25) Song, S. P.; Liang, Z. Q.; Zhang, J.; Wang, L. H.; Li, G. X.; Fan, C. H. Gold-Nanoparticle-Based Multicolor Nanobeacons for Sequence-Specific DNA Analysis. *Angew Chem Int Edit* **2009**, *48*, 8670-8674.

(26) Li, N.; Chang, C. Y.; Pan, W.; Tang, B. A Multicolor Nanoprobe for Detection and Imaging of Tumor-Related mRNAs in Living Cells. *Angew Chem Int Edit* **2012**, *51*, 7426-7430.

(27) Liu, J.; Lu, Y. Preparation of aptamer-linked gold nanoparticle purple aggregates for colorimetric sensing of analytes. *Nat Protoc* **2006**, *1*, 246-252.

(28) Hill, H. D.; Millstone, J. E.; Banholzer, M. J.; Mirkin, C. A. The Role Radius of Curvature Plays in Thiolated Oligonucleotide Loading on Gold Nanoparticles. *Acs Nano* **2009**, *3*, 418-424.

(29) Zhang, X.; Servos, M. R.; Liu, J. W. Instantaneous and Quantitative Functionalization of Gold Nanoparticles with Thiolated DNA Using a pH-Assisted and Surfactant-Free Route. *Journal of the American Chemical Society* **2012**, *134*, 7266-7269.

(30) Pei, H.; Zuo, X. L.; Zhu, D.; Huang, Q.; Fan, C. H. Functional DNA Nanostructures for Theranostic Applications. *Accounts Chem Res* **2014**, *47*, 550-559.

(31) Schreiner, S. M.; Shudy, D. F.; Hatch, A. L.; Opdahl, A.; Whitman, L. J.; Petrovykh, D. Y. Controlled and Efficient Hybridization Achieved with DNA Probes Immobilized Solely through Preferential DNA-Substrate Interactions. *Anal Chem* **2010**, *82*, 2803-2810.

(32) Opdahl, A.; Petrovykh, D. Y.; Kimura-Suda, H.; Tarlov, M. J.; Whitman, L. J. Independent control of grafting density and conformation of single-stranded DNA brushes. *P Natl Acad Sci USA* **2007**, *104*, 9-14.

(33) Pei, H.; Li, F.; Wan, Y.; Wei, M.; Liu, H.; Su, Y.; Chen, N.; Huang, Q.; Fan, C. Designed diblock oligonucleotide for the synthesis of spatially isolated and highly hybridizable functionalization of DNA-gold nanoparticle nanoconjugates. *Journal of the American Chemical Society* **2012**, *134*, 11876-11879.

(34) Yao, G. B.; Pei, H.; Li, J.; Zhao, Y.; Zhu, D.; Zhang, Y. N.; Lin, Y. F.; Huang, Q.; Fan, C. H. Clicking DNA to gold nanoparticles: poly-adenine-mediated formation of monovalent DNA-gold nanoparticle conjugates with nearly quantitative yield. *Npg Asia Mater* **2015**, *7*.

(35) Demers, L. M.; Mirkin, C. A.; Mucic, R. C.; Reynolds, R. A., 3rd; Letsinger, R. L.; Elghanian, R.; Viswanadham, G. A fluorescence-based method for determining the surface coverage and hybridization efficiency of thiol-capped oligonucleotides bound to gold thin films and nanoparticles. *Anal. Chem.* **2000**, *72*, 5535-5541.

(36) Mitchell, P. S.; Parkin, R. K.; Kroh, E. M.; Fritz, B. R.; Wyman, S. K.; Pogosova-Agadjanyan, E. L.; Peterson, A.; Noteboom, J.; O'Briant, K. C.; Allen, A.; Lin, D. W.; Urban, N.; Drescher, C. W.; Knudsen, B. S.; Stirewalt, D. L.; Gentleman, R.; Vessella, R. L.; Nelson, P. S.; Martin, D. B.; Tewari, M. Circulating microRNAs as stable blood-based markers for cancer detection. *P Natl Acad Sci USA* **2008**, *105*, 10513-10518.

(37) Wen, Y. L.; Pei, H.; Shen, Y.; Xi, J. J.; Lin, M. H.; Lu, N.; Shen, X. Z.; Li, J.; Fan, C. H. DNA Nanostructure-based Interfacial engineering for PCR-free ultrasensitive electrochemical analysis of microRNA (vol 2, pg 267, 2012). *Sci Rep-Uk* **2013**, *3*.

(38) Yang, L.; Liu, C. H.; Ren, W.; Li, Z. P. Graphene Surface-Anchored Fluorescence Sensor for Sensitive Detection of MicroRNA Coupled with Enzyme-Free Signal Amplification of Hybridization Chain Reaction. *Acs Appl Mater Inter* **2012**, *4*, 6450-6453.

(39) Duan, R. X.; Zuo, X. L.; Wang, S. T.; Quan, X. Y.; Chen, D. L.; Chen, Z. F.; Jiang, L.; Fan, C. H.; Xia, F. Quadratic isothermal amplification for the detection of microRNA. *Nat Protoc* **2014**, *9*, 597-607.

(40) Song, M. Y.; Pan, K. F.; Su, H. J.; Zhang, L.; Ma, J. L.; Li, J. Y.; Yuasa, Y.; Kang, D.; Kim, Y. S.; You, W. C. Identification of Serum MicroRNAs as Novel Non-Invasive Biomarkers for Early Detection of Gastric Cancer. *Plos One* **2012**, *7*.

(41) Wang, J.; Chen, J. Y.; Chang, P.; LeBlanc, A.; Li, D. H.; Abbruzzesse, J. L.; Frazier, M. L.; Killary, A. M.; Sen, S. MicroRNAs in Plasma of Pancreatic Ductal Adenocarcinoma Patients as Novel Blood-Based Biomarkers of Disease. *Cancer Prev Res* **2009**, *2*, 807-813.

(42) Habbe, N.; Koorstra, J. B. M.; Mendell, J. T.; Offerhaus, G. J.; Ryu, J. K.; Feldmann, G.; Mullendore, M. E.; Goggins, M. G.; Hong, S. M.; Maitra, A. MicroRNA miR-155 is a biomarker of early pancreatic neoplasia. *Cancer Biol Ther* **2009**, *8*, 340-346.

(43) Hill, H. D.; Mirkin, C. A. The bio-barcode assay for the detection of protein and nucleic acid targets using DTT-induced ligand exchange. *Nat Protoc* **2006**, *1*, 324-336.

(44) Alivisatos, A. P.; Johnsson, K. P.; Peng, X. G.; Wilson, T. E.; Loweth, C. J.; Bruchez, M. P.; Schultz, P. G. Organization of 'nanocrystal molecules' using DNA. *Nature* **1996**, *382*, 609-611.